Available online at www.sciencedirect.com
ScienceDirect
Journal of Sound and Vibration 314 (2008) 254–274
JOURNAL OF SOUND AND VIBRATION
www.elsevier.com/locate/jsvi

Vibration of post-buckled sandwich plates with FGM face sheets in a thermal environment

Xian-Kun Xia[a], Hui-Shen Shen[a,b,*]

[a]School of Ocean and Civil Engineering, Shanghai Jiao Tong University, Shanghai 200030, People's Republic of China
[b]State Key Laboratory of Ocean Engineering, Shanghai Jiao Tong University, Shanghai 200030, People's Republic of China

Received 17 May 2007; received in revised form 1 December 2007; accepted 4 January 2008
Handling Editor: L.G. Tham
Available online 20 February 2008

Abstract

This paper deals with the small- and large-amplitude vibrations of compressively and thermally post-buckled sandwich plates with functionally graded material (FGM) face sheets in thermal environments. Both heat conduction and temperature-dependent material properties are taken into account. The material properties of FGM face sheets are assumed to be graded in the thickness direction according to a simple power-law distribution in terms of the volume fractions of the constituents, and the material properties of both FGM face sheets and a homogeneous substrate are assumed to be temperature dependent. The formulations are based on a higher-order shear deformation plate theory and a general von Kármán-type equation that includes a thermal effect. The equations of motion are solved by an improved perturbation technique. The numerical illustrations concern small- and large-amplitude vibration characteristics of post-buckled sandwich plates with FGM face sheets under uniform and non-uniform temperature fields. The results show that, as the volume fraction index increases, the fundamental frequency increases in the pre-buckling region, but decreases in the post-buckling region. In contrast, the nonlinear frequency ratio decreases in both the pre- and post-buckling region on increasing the volume fraction index. The results also reveal that the substrate-to-face sheet thickness ratio and temperature changes have a significant effect on the fundamental frequency, but only have a small effect on the nonlinear frequency ratio.

1. Introduction

A typical laminated structure, which, due to its outstanding features, is used in the aeronautical industry, is the sandwich-type construction. Recently, sandwich construction has become even more attractive for the introduction of advanced composite materials for face sheets [1,2]. Functionally graded materials (FGMs) are microscopically inhomogeneous composites usually made from a mixture of metals and ceramics. The numerous advantages offered by FGMs over conventional materials and the need to overcome the technical

*Corresponding author at: School of Ocean and Civil Engineering, Shanghai Jiao Tong University, Shanghai 200030, People's Republic of China.
E-mail address: hsshen@mail.sjtu.edu.cn (H.-S. Shen).

0022-460X/$ - see front matter © 2008 Elsevier Ltd. All rights reserved.
doi:10.1016/j.jsv.2008.01.019

challenges involving high-temperature environments have prompted an increased use of sandwich structures with FGM facings.

A great deal of interest for the vibration analysis of post-buckled plates is being shown in the specialized literature. Bisplinghoff and Pian [3] studied the small-amplitude vibrations of a simply supported rectangular isotropic post-buckled plate with an aspect ratio of 3, subjected to in-plane compression due to thermal loading. In their analysis, the model equations of motion were derived from Lagrange's equation with the strain energy and kinetic energy. Yang and Han [4] studied the small- and large-amplitude vibration of isotropic post-buckled plates. In their analysis, a simple relation between the uniform temperature change and the in-plane compressive load in the post-buckling region was used. Zhou et al. [5] studied the free vibration of thermally buckled composite plates. The influence of lamination angle, temperature distribution, plate planform of arbitrary shape and boundary support conditions on post-buckling and vibration behavior was investigated. Lee and Lee [6,7] investigated vibration behaviors of unstiffened and stiffened, thermally post-buckled anisotropic plates using the first-order shear deformable plate theory. The effect of fiber orientation angle and aspect ratio on post-buckling and vibration behaviors was investigated for simply supported laminated plates subject to a steady-state uniform temperature increase. Shiau and Wu [8] studied free vibration of buckled composite plates and found that for a plate with certain boundary conditions, the natural frequency may show a sudden jump due to buckle pattern change of the plate in the post-buckling region. This work was then extended to the case of free vibration of thermally buckled sandwich plates with composite face sheets [9]. Their results show that if the shape of a free vibration mode is similar to the plate buckling mode then the natural frequency of that mode will drop to zero when the temperature reaches the buckling temperature. Girish and Ramachandra [10] presented the post-buckling and post-buckled vibrations of a symmetrically laminated composite plate subjected to a uniform temperature distribution through the thickness. The structural model is based on a higher-order shear deformation theory and the Galerkin method, along with Newton–Raphson procedure was used to solve nonlinear algebraic equations. The free vibration frequencies of a thermally post-buckled plate were reported by solving the eigenvalue problem for different post-buckled deflections. Singha et al. [11] analyzed the vibration characteristics of thermally stressed composite skew plates in the pre- and post-buckling states. Park and Kim [12] investigated thermal post-buckling and small-amplitude vibration behaviors of simply supported FGM plates with temperature-dependent material properties in the pre- and post-buckled regions. Their results show that the behaviors of the thermal post-buckling and vibration of the FGM plate are different from those of the isotropic plate, and the volume fraction of the constituent materials for FGMs has an effect on behaviors of the thermal post-buckling and vibration of the FGM plates. In the aforementioned investigations, nonlinear finite element equations based on a classical or a first-order shear deformation theory were formulated [4–9,11,12], but the material properties were assumed to be independent of temperature except for [12].

Since FGMs are used in high-temperature environments, the constituents of FGM face sheets possess temperature-dependent properties. Therefore, the material properties of FGM face sheets must be temperature dependent and position dependent. On the other hand, ceramics and metals used in FGMs do store different amounts of heat, and therefore heat conduction usually occurs. When the material properties are assumed to be functions of temperature and position, and the temperature is also assumed to be a function of position, the problem becomes very complicated.

The present work deals with the small- and large-amplitude vibrations of compressively and thermally post-buckled sandwich plates with FGM face sheets in thermal environments. The novel contribution of the present work is that both the heat conduction and temperature-dependent material properties are taken into account. The material properties of FGM face sheets are assumed to be graded in the thickness direction according to a simple power-law distribution in terms of the volume fractions of the constituents, and the material properties of both FGM face sheets and the homogeneous substrate are assumed to be temperature dependent. The formulations of the plate are based on Reddy's higher-order shear deformation plate theory that includes thermal effects. The von Kármán nonlinear strain–displacement relation is used to account for a large deflection. These equations can be mathematically divided into two sets and solved in sequence. The first set of equations yields the particular solution of static post-buckling or thermal post-buckling deflection, and the second set of equations gives the homogeneous solution of vibration characteristics on the buckled plate.

The numerical illustrations show the effect of temperature field, volume fraction distribution of FGM face sheets and substrate-to-face sheet thickness ratio on the vibration characteristics of sandwich plates.

2. Theoretical development

The sandwich plate considered herein comprises one homogeneous substrate and two face sheets made of FGMs and is mid-plane symmetric, as shown in Fig. 1. The length, width and thickness of the sandwich plate are a, b and h. The thickness of each FGM face sheet is h_F, while the thickness of the homogeneous substrate is h_H. The plate is subjected to a compressive edge load in the X-direction and/or thermal loading. As usual, the coordinate system has its origin at the corner of the plate on the mid-plane. Let $\bar{U}$, $\bar{V}$ and $\bar{W}$ be the plate displacements parallel to a right-hand set of axes (X, Y, Z), where X is longitudinal and Z is perpendicular to the plate. $\bar{\Psi}_x$ and $\bar{\Psi}_y$ are the mid-plane rotations of the normals about the Y and X axes, respectively. Let $\bar{F}(X, Y)$ be the stress function for the stress resultants defined by $\bar{N}_x = \bar{F}_{,yy}$, $\bar{N}_y = \bar{F}_{,xx}$ and $\bar{N}_{xy} = -\bar{F}_{,xy}$, where a comma denotes partial differentiation with respect to the corresponding coordinates.

The FGM face sheet is made from a mixture of ceramics and metals, the mixing ratio of which is varied continuously and smoothly in the Z direction. This is achieved by using a simple rule of mixture of composite materials. The accuracy of the rule of mixture was discussed and a remarkable synergism between the Mori–Tanaka scheme and the rule of mixture was found in Ref. [13]. The effective material properties P_f (like Young's modulus E_f or thermal expansion coefficient α_f) can be expressed as

$$P_f = P_c V_c + P_m V_m \tag{1}$$

in which P_c and P_m denote the temperature-dependent properties of the ceramic and metal, respectively, and V_c and V_m are the ceramic and metal volume fractions and are related by

$$V_c + V_m = 1. \tag{2}$$

The volume fraction V_m (for the top FGM face sheet) follows a simple power law as

$$V_m = \left(\frac{Z - h_0}{h_1 - h_0}\right)^N, \tag{3}$$

where the volume fraction index N ($0 \leqslant N \leqslant \infty$) dictates the material variation profile through the FGM layer thickness.

It is postulated that the effective Young's modulus E_f, thermal expansion coefficient α_f and thermal conductivity κ_f are temperature dependent, whereas the mass density ρ_f is independent of the temperature. Poisson's ratio v_f depends weakly on temperature change and is assumed to be a constant. From Eqs. (1) to (3), one has

$$E_f(Z, T) = [E_m(T) - E_c(T)]\left(\frac{Z - h_0}{h_1 - h_0}\right)^N + E_c(T), \tag{4a}$$

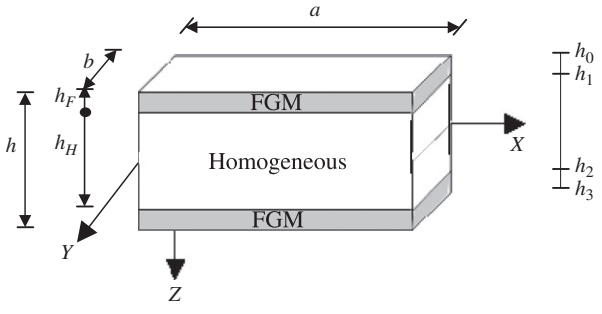

Fig. 1. Configuration of a sandwich plate.

$$\alpha_f(Z,T) = [\alpha_m(T) - \alpha_c(T)]\left(\frac{Z-h_0}{h_1-h_0}\right)^N + \alpha_c(T), \tag{4b}$$

$$\kappa_f(Z,T) = [\kappa_m(T) - \kappa_c(T)]\left(\frac{Z-h_0}{h_1-h_0}\right)^N + \kappa_c(T), \tag{4c}$$

$$\rho_f(Z) = (\rho_m - \rho_c)\left(\frac{Z-h_0}{h_1-h_0}\right)^N + \rho_c. \tag{4d}$$

We assume that the temperature variation occurs in the thickness direction only and the one-dimensional temperature field is assumed to be constant in the XY plane of the plate. In such a case, the temperature distribution along the thickness can be obtained by solving a steady-state heat transfer equation

$$-\frac{\mathrm{d}}{\mathrm{d}Z}\left[\kappa\frac{\mathrm{d}T}{\mathrm{d}Z}\right] = 0, \tag{5}$$

where

$$\kappa = \begin{cases} \kappa_f & (h_0 \leqslant Z < h_1), \\ \kappa_H & (h_1 \leqslant Z \leqslant h_2), \\ \kappa_f & (h_2 < Z \leqslant h_3), \end{cases} \tag{6a}$$

$$T = \begin{cases} T_f & (h_0 \leqslant Z \leqslant h_1), \\ T_H & (h_1 \leqslant Z \leqslant h_2), \\ \tilde{T}_f & (h_2 \leqslant Z \leqslant h_3), \end{cases} \tag{6b}$$

where κ_H is the thermal conductivity of the homogeneous substrate. Eq. (5) is solved by imposing the boundary conditions $T = T_U$ at $Z = h_0$ and $T = T_L$ at $Z = h_3$, and the continuity conditions

$$T_F(h_1) = T_H(h_1) = T_{m1}, \quad T_H(h_2) = \tilde{T}_F(h_2) = T_{m2}, \tag{7a}$$

$$\kappa_m\frac{\mathrm{d}T_F}{\mathrm{d}Z}\bigg|_{Z=h_1} = \kappa_H\frac{\mathrm{d}T_H}{\mathrm{d}Z}\bigg|_{Z=h_1}, \quad \kappa_H\frac{\mathrm{d}T_H}{\mathrm{d}Z}\bigg|_{Z=h_2} = \kappa_m\frac{\mathrm{d}\tilde{T}_F}{\mathrm{d}Z}\bigg|_{Z=h_2}, \tag{7b}$$

where T_U and T_L are the temperatures at the top and the bottom surfaces of the plate, and T_{m1} and T_{m2} are the temperatures at $Z = h_1$ and h_2 interfaces, respectively.

The solution of Eqs. (5)–(7), by means of polynomial series, is

$$T_F = T_U + (T_{m1} - T_U)\eta(Z), \tag{8a}$$

$$T_H = \frac{1}{h_H}[(T_{m1}h_2 - T_{m2}h_1) + (T_{m2} - T_{m1})Z], \tag{8b}$$

$$\tilde{T}_F(Z) = T_L + (T_{m2} - T_L)\tilde{\eta}(Z) \tag{8c}$$

in which

$$\eta(Z) = \frac{1}{C}\left[\left(\frac{Z-h_0}{h_1-h_0}\right) - \frac{\kappa_{mc}}{(N+1)\kappa_c}\left(\frac{Z-h_0}{h_1-h_0}\right)^{N+1} + \frac{\kappa_{mc}^2}{(2N+1)\kappa_c^2}\left(\frac{Z-h_0}{h_1-h_0}\right)^{2N+1}\right.$$
$$\left. - \frac{\kappa_{mc}^3}{(3N+1)\kappa_c^3}\left(\frac{Z-h_0}{h_1-h_0}\right)^{3N+1} + \frac{\kappa_{mc}^4}{(4N+1)\kappa_c^4}\left(\frac{Z-h_0}{h_1-h_0}\right)^{4N+1} - \frac{\kappa_{mc}^5}{(5N+1)\kappa_c^5}\left(\frac{Z-h_0}{h_1-h_0}\right)^{5N+1}\right], \tag{9a}$$

$$\tilde{\eta}(Z)=\frac{1}{C}\left[\left(\frac{Z-h_3}{h_2-h_3}\right)-\frac{\kappa_{mc}}{(N+1)\kappa_c}\left(\frac{Z-h_3}{h_2-h_3}\right)^{N+1}+\frac{\kappa_{mc}^2}{(2N+1)\kappa_c^2}\left(\frac{Z-h_3}{h_2-h_3}\right)^{2N+1}\right.$$
$$\left.-\frac{\kappa_{mc}^3}{(3N+1)\kappa_c^3}\left(\frac{Z-h_3}{h_2-h_3}\right)^{3N+1}+\frac{\kappa_{mc}^4}{(4N+1)\kappa_c^4}\left(\frac{Z-h_3}{h_2-h_3}\right)^{4N+1}-\frac{\kappa_{mc}^5}{(5N+1)\kappa_c^5}\left(\frac{Z-h_3}{h_2-h_3}\right)^{5N+1}\right], \tag{9b}$$

$$C=1-\frac{\kappa_{mc}}{(N+1)\kappa_c}+\frac{\kappa_{mc}^2}{(2N+1)\kappa_c^2}-\frac{\kappa_{mc}^3}{(3N+1)\kappa_c^3}+\frac{\kappa_{mc}^4}{(4N+1)\kappa_c^4}-\frac{\kappa_{mc}^5}{(5N+1)\kappa_c^5}, \tag{9c}$$

$$G=1-\frac{\kappa_{mc}}{\kappa_c}+\frac{\kappa_{mc}^2}{\kappa_c^2}-\frac{\kappa_{mc}^3}{\kappa_c^3}+\frac{\kappa_{mc}^4}{\kappa_c^4}-\frac{\kappa_{mc}^5}{\kappa_c^5},$$

where $\kappa_{mc}=\kappa_m-\kappa_c$, and

$$T_{m1}=\frac{[(\kappa_H/h_H)+(\kappa_m G/t_F C)]T_U+(\kappa_H/h_H)T_L}{(\kappa_m G/h_F C)+(2\kappa_H/h_H)},\quad T_{m2}=\frac{[(\kappa_H/h_H)+(\kappa_m G/h_F C)]T_L+(\kappa_H/h_H)T_U}{(\kappa_m G/h_F C)+(2\kappa_H/h_H)}. \tag{10}$$

Note that in the above equations κ_H, κ_m and κ_c are temperature dependent.

Reddy [14,15] developed a simple higher-order shear deformation plate theory, in which the transverse shear strains are assumed to be parabolically distributed across the plate thickness and which contains the same dependent unknowns ($\bar{U}$, $\bar{V}$, $\bar{W}$, $\bar{\Psi}_x$ and $\bar{\Psi}_y$) as in the first-order shear deformation theory, but no shear correction factors are required. Based on Reddy's higher-order shear deformation plate theory, Shen [16] derived a set of general von Kármán-type equations which can be expressed in terms of a transverse displacement $\bar{W}$, two rotations $\bar{\Psi}_x$ and $\bar{\Psi}_y$ and stress function $\bar{F}$. These general von Kármán-type equations are successfully used in solving many nonlinear problems, e.g. nonlinear bending, post-buckling and nonlinear vibration of shear deformable FGM plates [17–19]. By using Hamilton's principle, we can easily obtain the nonlinear motion equations of such plates as [19]

$$\tilde{L}_{11}(\bar{W})-\tilde{L}_{12}(\bar{\Psi}_x)-\tilde{L}_{13}(\bar{\Psi}_y)+\tilde{L}_{14}(\bar{F})-\tilde{L}_{15}(\bar{N}^{\mathrm{T}})-\tilde{L}_{16}(\bar{M}^{\mathrm{T}})$$
$$=\tilde{L}(\bar{W},\bar{F})+\tilde{L}_{17}(\ddot{\bar{W}})+I_8\left(\frac{\partial\ddot{\bar{\Psi}}_x}{\partial X}+\frac{\partial\ddot{\bar{\Psi}}_y}{\partial Y}\right), \tag{11}$$

$$\tilde{L}_{21}(\bar{F})+\tilde{L}_{22}(\bar{\Psi}_x)+\tilde{L}_{23}(\bar{\Psi}_y)-\tilde{L}_{24}(\bar{W})-\tilde{L}_{25}(\bar{N}^{\mathrm{T}})=-\tfrac{1}{2}\tilde{L}(\bar{W},\bar{W}), \tag{12}$$

$$\tilde{L}_{31}(\bar{W})+\tilde{L}_{32}(\bar{\Psi}_x)-\tilde{L}_{33}(\bar{\Psi}_y)+\tilde{L}_{34}(\bar{F})-\tilde{L}_{35}(\bar{N}^{\mathrm{T}})-\tilde{L}_{36}(\bar{S}^{\mathrm{T}})=I_9\frac{\partial\ddot{\bar{W}}}{\partial X}+I_{10}\ddot{\bar{\Psi}}_x, \tag{13}$$

$$\tilde{L}_{41}(\bar{W})-\tilde{L}_{42}(\bar{\Psi}_x)+\tilde{L}_{43}(\bar{\Psi}_y)+\tilde{L}_{44}(\bar{F})-\tilde{L}_{45}(\bar{N}^{\mathrm{T}})-\tilde{L}_{46}(\bar{S}^{\mathrm{T}})=I_9\frac{\partial\ddot{\bar{W}}}{\partial Y}+I_{10}\ddot{\bar{\Psi}}_y \tag{14}$$

in which I_j and $\bar{I}_j$ are defined as in Huang and Zheng [20], and the linear operators $\tilde{L}_{ij}(\cdot)$ and the nonlinear operator $\tilde{L}(\,)$ are defined as in Shen [21]. Note that the geometric nonlinearity in the von Kármán sense is given in terms of $\tilde{L}(\,)$ in Eqs. (11) and (12).

Since the material properties are assumed to be a functions of T and Z, and the temperature is also assumed to be function of Z, even for the mid-plane symmetric plate the coupling between transverse bending and in-plane stretching which is given in terms of B_{ij}^* and $E_{ij}^*(i,j=1,2,6)$ still exists when the plate is subjected to heat conduction. In contrast, when the plate is subjected to a uniform temperature increase, all B_{ij}^* and E_{ij}^* are zero valued.

In the above equations, the superposed dots indicate differentiation with respect to time. The forces $\bar{N}^{\mathrm{T}}$, moments $\bar{M}^{\mathrm{T}}$and higher-order moments $\bar{P}^{\mathrm{T}}$ and $\bar{S}^{\mathrm{T}}$ caused by temperature increase are

defined by

$$\begin{bmatrix} \bar{N}_x^T & \bar{M}_x^T & \bar{P}_x^T \\ \bar{N}_y^T & \bar{M}_y^T & \bar{P}_y^T \\ \bar{N}_{xy}^T & \bar{M}_{xy}^T & \bar{P}_{xy}^T \end{bmatrix} = \sum_{k=1} \int_{h_{k-1}}^{h_k} \begin{bmatrix} A_x \\ A_y \\ A_{xy} \end{bmatrix}_k (1, Z, Z^3) \Delta T(Z)\, dZ, \tag{15a}$$

$$\begin{bmatrix} \bar{S}_x^T \\ \bar{S}_y^T \\ \bar{S}_{xy}^T \end{bmatrix} = \begin{bmatrix} \bar{M}_x^T \\ \bar{M}_y^T \\ \bar{M}_{xy}^T \end{bmatrix} - \frac{4}{3h^2} \begin{bmatrix} \bar{P}_x^T \\ \bar{P}_y^T \\ \bar{P}_{xy}^T \end{bmatrix}, \tag{15b}$$

where $\Delta T(Z) = T(Z) - T_0$ is the temperature increase from the reference temperature T_0 at which there are no thermal strains, and

$$\begin{bmatrix} A_x \\ A_y \\ A_{xy} \end{bmatrix} = - \begin{bmatrix} \bar{Q}_{11} & \bar{Q}_{12} & \bar{Q}_{16} \\ \bar{Q}_{12} & \bar{Q}_{22} & \bar{Q}_{26} \\ \bar{Q}_{16} & \bar{Q}_{26} & \bar{Q}_{66} \end{bmatrix} \begin{bmatrix} 1 & 0 \\ 0 & 1 \\ 0 & 0 \end{bmatrix} \begin{bmatrix} \alpha_{11} \\ \alpha_{22} \end{bmatrix} \tag{16}$$

in which α_{11} and α_{22} are the thermal expansion coefficients measured in the longitudinal and transverse directions, respectively, and $\bar{Q}_{ij}$ are the transformed elastic constants, details of which can be found in Refs. [14,15]. Note that for an FGM face sheet, $\alpha_{11} = \alpha_{22} = \alpha_f$ is given in detail in Eq. (4), and $\bar{Q}_{ij} = Q_{ij}$ in which

$$Q_{11} = Q_{22} = \frac{E_f(Z,T)}{1 - v_f^2}, \quad Q_{12} = \frac{v_f E_f(Z,T)}{1 - v_f^2}, \quad Q_{16} = Q_{26} = 0, \quad Q_{44} = Q_{55} = Q_{66} = \frac{E_f(Z,T)}{2(1 + v_f)}, \tag{17}$$

where E_f is also given in detail in Eq. (4).

All four edges of the plate are assumed to be simply supported. Depending on the in-plane behavior at the edges, two cases, Case 1 (for the compressively buckled plate) and Case 2 (for the thermally buckled plate), will be considered. They are as follows.

Case 1: The edges are simply supported and freely movable in the in-plane directions. In addition the plate is subjected to uniaxial compressive edge loads.

Case 2: All four edges are simply supported with no in-plane displacements, i.e. prevented from moving in the X- and Y-direction.

For both cases, the associated boundary conditions can be expressed as

$X = 0, a$:

$$\bar{W} = \bar{\Psi}_y = 0, \tag{18a}$$

$$\bar{M}_x = \bar{P}_x = 0, \tag{18b}$$

$$\int_0^b \bar{N}_x\, dY + P = 0 \quad \text{(for a compressively buckled plate)}, \tag{18c}$$

$$\bar{U} = 0 \quad \text{(for a thermally buckled plate)}, \tag{18d}$$

$Y = 0, b$:

$$\bar{W} = \bar{\Psi}_x = 0, \tag{18e}$$

$$\bar{M}_y = \bar{P}_y = 0, \tag{18f}$$

$$\int_0^a \bar{N}_y\, dX = 0 \quad \text{(for a compressively buckled plate)}, \tag{18g}$$

$$\bar{V} = 0 \quad \text{(for a thermally buckled plate)}, \tag{18h}$$

where P is a compressive edge load in the X-direction, $\bar{M}_x$ and $\bar{M}_y$ are the bending moments and $\bar{P}_x$ and $\bar{P}_y$ are the higher-order moments as defined in Refs. [14,15].

The average end-shortening relationships are

$$\begin{aligned}\frac{\Delta_x}{a} &= -\frac{1}{ab}\int_0^b\int_0^a \frac{\partial \bar{U}}{\partial X}\,\mathrm{d}X\,\mathrm{d}Y \\ &= -\frac{1}{ab}\int_0^b\int_0^a \left[A_{11}^*\frac{\partial^2\bar{F}}{\partial Y^2} + A_{12}^*\frac{\partial^2\bar{F}}{\partial X^2} + \left(B_{11}^* - \frac{4}{3h^2}E_{11}^*\right)\frac{\partial\bar{\Psi}_x}{\partial X} + \left(B_{12}^* - \frac{4}{3h^2}E_{12}^*\right)\frac{\partial\bar{\Psi}_y}{\partial Y}\right. \\ &\quad \left. -\frac{4}{3h^2}\left(E_{11}^*\frac{\partial^2\bar{W}}{\partial X^2} + E_{12}^*\frac{\partial^2\bar{W}}{\partial Y^2}\right) - \frac{1}{2}\left(\frac{\partial\bar{W}}{\partial X}\right)^2 - (A_{11}^*\bar{N}_x^{\mathrm{T}} + A_{12}^*\bar{N}_y^{T})\right]\mathrm{d}X\,\mathrm{d}Y,\end{aligned} \tag{19a}$$

$$\begin{aligned}\frac{\Delta_y}{b} &= -\frac{1}{ab}\int_0^a\int_0^b \frac{\partial \bar{V}}{\partial Y}\,\mathrm{d}Y\,\mathrm{d}X \\ &= -\frac{1}{ab}\int_0^a\int_0^b \left[A_{22}^*\frac{\partial^2\bar{F}}{\partial X^2} + A_{12}^*\frac{\partial^2\bar{F}}{\partial Y^2} + \left(B_{21}^* - \frac{4}{3h^2}E_{21}^*\right)\frac{\partial\bar{\Psi}_x}{\partial X} + \left(B_{22}^* - \frac{4}{3h^2}E_{22}^*\right)\frac{\partial\bar{\Psi}_y}{\partial Y}\right. \\ &\quad \left. -\frac{4}{3h^2}\left(E_{21}^*\frac{\partial^2\bar{W}}{\partial X^2} + E_{22}^*\frac{\partial^2\bar{W}}{\partial Y^2}\right) - \frac{1}{2}\left(\frac{\partial\bar{W}}{\partial Y}\right)^2 - (A_{12}^*\bar{N}_x^{\mathrm{T}} + A_{22}^*\bar{N}_y^{\mathrm{T}})\right]\mathrm{d}Y\,\mathrm{d}X,\end{aligned} \tag{19b}$$

where Δ_x and Δ_y are plate end-shortening displacements in the X- and Y-direction.

In the above equations and what follows, the reduced stiffness matrices $[A_{ij}^*]$, $[B_{ij}^*]$, $[D_{ij}^*]$, $[E_{ij}^*]$, $[F_{ij}^*]$ and $[H_{ij}^*]$ $(i,j = 1, 2, 6)$ are functions of T and Z, determined through relationships [16]

$$\mathbf{A}^* = \mathbf{A}^{-1}, \quad \mathbf{B}^* = -\mathbf{A}^{-1}\mathbf{B}, \quad \mathbf{D}^* = \mathbf{D} - \mathbf{B}\mathbf{A}^{-1}\mathbf{B}, \quad \mathbf{E}^* = -\mathbf{A}^{-1}\mathbf{E}, \quad \mathbf{F}^* = \mathbf{F} - \mathbf{E}\mathbf{A}^{-1}\mathbf{B}, \quad \mathbf{H}^* = \mathbf{H} - \mathbf{E}\mathbf{A}^{-1}\mathbf{E}, \tag{20}$$

where A_{ij}, B_{ij}, etc., are the plate stiffnesses, defined by

$$(A_{ij}, B_{ij}, D_{ij}, E_{ij}, F_{ij}, H_{ij}) = \sum_k \int_{h_{k-1}}^{h_k} (\mathrm{Q}_{ij})_k (1, Z, Z^2, Z^3, Z^4, Z^6)\,\mathrm{d}Z \quad (i,j = 1,2,6), \tag{21a}$$

$$(A_{ij}, D_{ij}, F_{ij}) = \sum_k \int_{h_{k-1}}^{h_k} (\mathrm{Q}_{ij})_k (1, Z^2, Z^4)\,\mathrm{d}Z \quad (i,j = 4,5). \tag{21b}$$

3. Analytical method and asymptotic solutions

Having developed the theory, we will try to solve Eqs. (11)–(14) with boundary condition (18). Before proceeding, it is convenient first to define the following dimensionless quantities:

$$x = \pi X/a, \quad y = \pi Y/b, \quad \beta = a/b, \quad W = \bar{W}/\left[D_{11}^* D_{22}^* A_{11}^* A_{22}^*\right]^{1/4},$$

$$F = \bar{F}/\left[D_{11}^* D_{22}^*\right]^{1/2}, \quad (\Psi_x, \Psi_y) = (\bar{\Psi}_x, \bar{\Psi}_y)a/\pi\left[D_{11}^* D_{22}^* A_{11}^* A_{22}^*\right]^{1/4}, \quad \gamma_5 = -A_{12}^*/A_{22}^*$$

$$\gamma_{14} = \left[D_{22}^*/D_{11}^*\right]^{1/2}, \quad \gamma_{24} = \left[A_{11}^*/A_{22}^*\right]^{1/2}, \quad (\gamma_{T1}, \gamma_{T2}) = \left(A_X^T, A_y^T\right)a^2/\pi^2\left[D_{11}^* D_{22}^*\right]^{1/2}$$

$$(\gamma_{T3}, \gamma_{T4}, \gamma_{T6}, \gamma_{T7}) = (D_x^{\mathrm{T}}, D_y^{\mathrm{T}}, F_x^{\mathrm{T}}, F_y^{\mathrm{T}})a^2/\pi^2 h^2 D_{11}^*$$

$$(M_x, M_y, P_x, P_y, M_x^{\mathrm{T}}, M_y^{\mathrm{T}}, P_x^{\mathrm{T}}, P_y^{\mathrm{T}}) = (\bar{M}_x, \bar{M}_y, 4\bar{P}_x/3h^2, 4\bar{P}_y/3h^2, \bar{M}_x^{\mathrm{T}}, \bar{M}_y^{\mathrm{T}}, 4\bar{P}_x^{\mathrm{T}}/3h^2, 4\bar{P}_y^{\mathrm{T}}/3h^2)a^2/\pi^2 D_{11}^*[D_{11}^* D_{22}^* A_{11}^* A_{22}^*]^{1/4},$$

$$\tau=\frac{\pi t}{a}\sqrt{\frac{E_0}{\rho_0}},\quad \gamma_{170}=-\frac{I_1E_0a^2}{\pi^2\rho_0D_{11}^*},\quad \gamma_{170}=-\frac{I_1E_0a^2}{\pi^2\rho_0D_{11}^*},\quad \gamma_{171}=\frac{4E_0(I_5I_1-I_4I_2)}{3\rho_0h^2I_1D_{11}^*}\quad \lambda_T=\alpha_0\Delta T_1,$$
$$(\gamma_{80},\gamma_{90},\gamma_{10})=(I_8,I_9,I_{10})\frac{E_0}{\rho_0D_{11}^*},\quad \lambda_x=Pb/4\pi^2\left[D_{11}^*D_{22}^*\right]^{1/2}, \tag{22}$$

in which α_0 is an arbitrary reference value defined by

$$\alpha_{11}=a_{11}\alpha_0,\quad \alpha_{22}=a_{22}\alpha_0 \tag{23}$$

and E_0 and ρ_0 are the reference values of E_m and ρ_m at room temperature ($T_0=300\,\mathrm{K}$), respectively, and $A_x^{\mathrm{T}}\left(=A_y^{\mathrm{T}}\right)$, $D_x^{\mathrm{T}}\left(=D_y^{\mathrm{T}}\right)$ and $F_x^{\mathrm{T}}\left(=F_y^{\mathrm{T}}\right)$ are defined by

$$\begin{bmatrix}A_x^{\mathrm{T}} & D_x^{\mathrm{T}} & F_x^{\mathrm{T}}\\ A_y^{\mathrm{T}} & D_y^{\mathrm{T}} & F_y^{\mathrm{T}}\end{bmatrix}\Delta T_1=-\sum_k\int_{h_{k-1}}^{h_k}\begin{bmatrix}A_x\\A_y\end{bmatrix}_k(1,Z,Z^3)\Delta T(Z)\,\mathrm{d}Z, \tag{24}$$

where ΔT_1 is a constant and is defined by $\Delta T_1=T_U-T_0$ for heat conduction.

Eqs. (11)–(14) may then be rewritten in the following dimensionless form:

$$L_{11}(W)-L_{12}(\Psi_x)-L_{13}(\Psi_y)+\gamma_{14}L_{14}(F)-L_{16}(M^{\mathrm{T}})=\gamma_{14}\beta^2L(W,F)+L_{17}(\ddot{W})+\gamma_{80}\left(\frac{\partial\ddot{\Psi}_x}{\partial x}+\beta\frac{\partial\ddot{\Psi}_y}{\partial y}\right), \tag{25}$$

$$L_{21}(F)+\gamma_{24}L_{22}(\Psi_x)+\gamma_{24}L_{23}(\Psi_y)-\gamma_{24}L_{24}(W)=-\tfrac{1}{2}\gamma_{24}\beta^2L(W,W), \tag{26}$$

$$L_{31}(W)+L_{32}(\Psi_x)-L_{33}(\Psi_y)+\gamma_{14}L_{34}(F)-L_{36}(S^T)=\gamma_{90}\frac{\partial\ddot{W}}{\partial x}+\gamma_{10}\ddot{\Psi}_x, \tag{27}$$

$$L_{41}(W)-L_{42}(\Psi_x)+L_{43}(\Psi_y)+\gamma_{14}L_{44}(F)-L_{46}(S^T)=\gamma_{90}\beta\frac{\partial\ddot{W}}{\partial y}+\gamma_{10}\ddot{\Psi}_y, \tag{28}$$

where the dimensionless operators $L_{ij}(\ )$ and $L(\ )$ are defined as in Ref. [17].

The boundary conditions of Eq. (18) become

$x=0,\ \pi$:

$$W=\Psi_y=0, \tag{29a}$$

$$M_x=P_x=0, \tag{29b}$$

$$\frac{1}{\pi}\int_0^{\pi}\beta^2\frac{\partial^2F}{\partial y^2}\,\mathrm{d}y+4\lambda_x\beta^2=0\quad\text{(for a compressively buckled plate)}, \tag{29c}$$

$$\delta_x=0\quad\text{(for a thermally buckled plate)}. \tag{29d}$$

$y=0,\ \pi$:

$$W=\Psi_x=0, \tag{29e}$$

$$M_y=P_y=0, \tag{29f}$$

$$\int_0^{\pi}\frac{\partial^2F}{\partial x^2}\,\mathrm{d}x=0\quad\text{(for a compressively buckled plate)}, \tag{29g}$$

$$\delta_y=0\quad\text{(for a thermally buckled plate)} \tag{29h}$$

and the unit end-shortening relationships become

$$\delta_x = -\frac{1}{4\pi^2\beta^2\gamma_{24}}\int_0^\pi\int_0^\pi\left[\gamma_{24}^2\beta^2\frac{\partial^2 F}{\partial y^2}-\gamma_5\frac{\partial^2 F}{\partial x^2}+\gamma_{24}\left(\gamma_{511}\frac{\partial \Psi_x}{\partial x}+\gamma_{233}\beta\frac{\partial \Psi_y}{\partial y}\right)\right.$$
$$\left.-\gamma_{24}\left(\gamma_{611}\frac{\partial^2 W}{\partial x^2}+\gamma_{244}\beta^2\frac{\partial^2 W}{\partial y^2}\right)-\frac{1}{2}\gamma_{24}\left(\frac{\partial W}{\partial x}\right)^2+(\gamma_{24}^2\gamma_{T1}-\gamma_5\gamma_{T2})\lambda_T\right]\mathrm{d}x\,\mathrm{d}y=0, \tag{30a}$$

$$\delta_y = -\frac{1}{4\pi^2\beta^2\gamma_{24}}\int_0^\pi\int_0^\pi\left[\frac{\partial^2 F}{\partial x^2}-\gamma_5\beta^2\frac{\partial^2 F}{\partial y^2}+\gamma_{24}\left(\gamma_{220}\frac{\partial \Psi_x}{\partial x}+\gamma_{522}\beta\frac{\partial \Psi_y}{\partial y}\right)\right.$$
$$\left.-\gamma_{24}\left(\gamma_{240}\frac{\partial^2 W}{\partial x^2}+\gamma_{622}\beta^2\frac{\partial^2 W}{\partial y^2}\right)-\frac{1}{2}\gamma_{24}\beta^2\left(\frac{\partial W}{\partial y}\right)^2+(\gamma_{T2}-\gamma_5\gamma_{T1})\lambda_T\right]\mathrm{d}y\,\mathrm{d}x=0. \tag{30b}$$

We assume that the solution of Eqs. (25)–(28) can be expressed as

$$\begin{aligned} W(x,y,\tau) &= W^*(x,y)+\tilde{W}(x,y,\tau),\\ \Psi_x(x,y,\tau) &= \Psi_x^*(x,y)+\tilde{\Psi}_x(x,y,\tau),\\ \Psi_y(x,y,\tau) &= \Psi_y^*(x,y)+\tilde{\Psi}_y(x,y,\tau),\\ F(x,y,\tau) &= F^*(x,y)+\tilde{F}(x,y,\tau), \end{aligned} \tag{31}$$

where $W^*(x, y)$ is an initial time-independent deflection due to prebuckling and post-buckling equilibrium states of sandwich plates subjected to uniaxial compression and/or thermal loading. $\Psi_x^*(x,y)$, $\Psi_y^*(x,y)$ and $F^*(x, y)$ are the mid-plane rotations and stress function corresponding to $W^*(x, y)$. $\tilde{W}(x,y,\tau)$ is an additional time-dependent displacement which is considered to originate from the linear or nonlinear vibration of sandwich plates. $\tilde{\Psi}_x(x,y,\tau)$,$\tilde{\Psi}_y(x,y,\tau)$ and $\tilde{F}(x,y,\tau)$ are defined analogously to $\Psi_x^*(x,y)$, $\Psi_y^*(x,y)$ and $F^*(x, y)$, but is for $\tilde{W}(x,y,\tau)$.

Substituting Eq. (31) into Eqs. (25)–(28), we obtain two sets of equations and can be solved in sequence. The first set of equations yields the particular solution of static post-buckling or thermal post-buckling deflection, and the second set of equations gives the homogeneous solution of vibration characteristics on the buckled plate.

As has been shown in Ref. [21], the solutions $W^*(x, y)$, $\Psi_x^*(x,y)$, $\Psi_y^*(x,y)$ and $F^*(x, y)$ may be expressed as

$$W^* = \varepsilon[A_{11}^{(1)}\sin kx\sin ly]+\varepsilon^3[A_{13}^{(3)}\sin kx\sin 3ly+A_{31}^{(3)}\sin 3k\sin ly]+O(\varepsilon^5), \tag{32}$$

$$F^* = -B_{00}^{(0)}\frac{y^2}{2}-b_{00}^{(0)}\frac{x^2}{2}+\varepsilon^2\left[-B_{00}^{(2)}\frac{y^2}{2}-b_{00}^{(2)}\frac{x^2}{2}+B_{20}^{(2)}\cos 2kx+B_{02}^{(2)}\cos 2ly\right]$$
$$+\varepsilon^4\left[-B_{00}^{(4)}\frac{y^2}{2}-b_{00}^{(4)}\frac{x^2}{2}+B_{20}^{(4)}\cos 2kx+B_{02}^{(4)}\cos 2ly+B_{22}^{(4)}\cos 2kx\cos 2ly\right.$$
$$\left.+B_{40}^{(4)}\cos 4kx+B_{04}^{(4)}\cos 4ly+B_{24}^{(4)}\cos 2kx\cos 4ly+B_{42}^{(4)}\cos 4kx\cos 2ly\right]+O(\varepsilon^5), \tag{33}$$

$$\Psi_x^* = \varepsilon[C_{11}^{(1)}\cos kx\sin ly]+\varepsilon^3[C_{13}^{(3)}\cos kx\sin 3ly+C_{31}^{(3)}\cos 3kx\sin ly]+O(\varepsilon^5), \tag{34}$$

$$\Psi_y^* = \varepsilon[D_{11}^{(1)}\sin kx\cos ly]+\varepsilon^3[D_{13}^{(3)}\sin kx\cos 3ly+D_{31}^{(3)}\sin 3kx\cos ly]+O(\varepsilon^5). \tag{35}$$

It is mentioned that all coefficients in Eqs. (32)–(35) are related and can be expressed in terms of $A_{11}^{(1)}$; the detailed expressions may be found in Ref. [22].

Then $\tilde{W}(x,y,\tau)$, $\tilde{\Psi}_x(x,y,\tau)$, $\tilde{\Psi}_y(x,y,\tau)$, $\tilde{F}(x,y,\tau)$ satisfy the nonlinear motion equations

$$L_{11}(\tilde{W}) - L_{12}(\tilde{\Psi}_x) - L_{13}(\tilde{\Psi}_y) + \gamma_{14}L_{14}(\tilde{F}) = \gamma_{14}\beta^2\left[L(\tilde{W}+W^*,\tilde{F}) + L(\tilde{W},F^*)\right] + L_{17}\left(\ddot{\tilde{W}}\right) + \gamma_{80}\left(\frac{\partial\ddot{\tilde{\Psi}}_x}{\partial x} + \beta\frac{\partial\ddot{\tilde{\Psi}}_y}{\partial y}\right), \tag{36}$$

$$L_{21}(\tilde{F}) + \gamma_{24}L_{22}(\tilde{\Psi}_x) + \gamma_{24}L_{23}(\tilde{\Psi}_y) - \gamma_{24}L_{24}(\tilde{W}) = -\tfrac{1}{2}\gamma_{24}\beta^2 L(\tilde{W}+2W^*,\tilde{W}), \tag{37}$$

$$L_{31}(\tilde{W}) + L_{32}(\tilde{\Psi}_x) - L_{33}(\tilde{\Psi}_y) + \gamma_{14}L_{34}(\tilde{F}) = \gamma_{90}\frac{\partial\ddot{\tilde{W}}}{\partial x} + \gamma_{10}\ddot{\tilde{\Psi}}_x \tag{38}$$

$$L_{41}(\tilde{W}) - L_{42}(\tilde{\Psi}_x) + L_{43}(\tilde{\Psi}_y) + \gamma_{14}L_{44}(\tilde{F}) = \gamma_{90}\beta\frac{\partial\ddot{\tilde{W}}}{\partial y} + \gamma_{10}\ddot{\tilde{\Psi}}_y. \tag{39}$$

It is assumed that the solutions of Eqs. (36)–(39) can be taken in the forms of perturbation expansions as

$$\tilde{W}(x,y,\tilde{\tau},\varepsilon) = \sum_{j=1}\varepsilon^j w_j(x,y,\tilde{\tau}), \quad \tilde{F}(x,y,\tilde{\tau},\varepsilon) = \sum_{j=0}\varepsilon^j f_j(x,y,\tilde{\tau}),$$
$$\tilde{\Psi}_x(x,y,\tilde{\tau},\varepsilon) = \sum_{j=1}\varepsilon^j \Psi_{xj}(x,y,\tilde{\tau}), \quad \tilde{\Psi}_y(x,y,\tilde{\tau},\varepsilon) = \sum_{j=1}\varepsilon^j \Psi_{yj}(x,y,\tilde{\tau}). \tag{40}$$

Here, we introduce an important parameter $\tilde{\tau} = \varepsilon\tau$, in which ε is a small parameter. Substituting Eq. (40) into Eqs. (36)–(39), and collecting terms of the same order of ε, a set of perturbation equations are obtained. Solving these equations step be step, we obtain asymptotic solutions, up to third order, as

$$\tilde{W}(x,y,\tau) = \varepsilon[w_1(\tau) + g_1\ddot{w}_1(\tau)]\sin mx\,\sin ny + (\varepsilon w_1(\tau))^3[g_{331}\sin 3mx\,\sin ny + g_{313}\sin mx\,\sin 3ny] + O(\varepsilon^4), \tag{41}$$

$$\tilde{F}(x,y,\tau) = \varepsilon[g_{31}^{(1,1)}w_1(\tau) + g_4\ddot{w}_1(\tau)]\sin mx\,\sin ny + (\varepsilon w_1(\tau))^2(g_{402}\cos 2ny + g_{420}\cos 2mx) + (\varepsilon w_1(\tau))^3[g_{31}^{(3,1)}g_{331}\sin 3mx\,\sin ny + g_{31}^{(1,3)}g_{313}\sin mx\,\sin 3ny] + O(\varepsilon^4), \tag{42}$$

$$\tilde{\Psi}_x(x,y,\tau) = \varepsilon[g_{11}^{(1,1)}w_1(\tau) + g_2\ddot{w}_1(\tau)]\cos mx\,\sin ny + (\varepsilon w_1(\tau))^2 g_{12}\sin 2mx + (\varepsilon w_1(\tau))^3[g_{11}^{(3,1)}g_{331}\cos 3mx\,\sin ny + g_{11}^{(1,3)}g_{313}\cos mx\,\sin 3ny] + O(\varepsilon^4) \tag{43}$$

$$\tilde{\Psi}_y(x,y,\tau) = \varepsilon[g_{21}^{(1,1)}w_1(\tau) + g_3\ddot{w}_1(\tau)]\sin mx\,\cos ny + (\varepsilon w_1(\tau))^2 g_{22}\sin 2ny + (\varepsilon w_1(\tau))^3[g_{21}^{(3,1)}g_{331}\sin 3mx\,\cos ny + g_{21}^{(1,3)}g_{313}\sin mx\,\cos 3ny] + O(\varepsilon^4). \tag{44}$$

Note that in Eqs. (41)–(44) $\tilde{\tau}$ is replaced by τ. Coefficients $g_{11}^{(i,j)}$, $g_{21}^{(i,j)}$, $g_{31}^{(i,j)}$ $(i,j=1,3)$, etc. are given in detail in the appendix. Also, we have

$$\begin{aligned}&\varepsilon[g_{41}w_1(\tau) + g_{43}\ddot{w}_1(\tau)]\sin mx\,\sin ny + (\varepsilon w_1(\tau))^2(g_{441}\cos 2mx + g_{442}\cos 2ny)\\ &+\gamma_{14}\beta^2(\varepsilon w_1(\tau))^2(\varepsilon A_{11}^{(1)})(4k^2n^2g_{402}\cos 2ny + 4l^2m^2g_{420}\cos 2mx)\sin kx\,\sin ly\\ &+\gamma_{14}\beta^2(\varepsilon w_1(\tau))^2(\varepsilon^3 A_{13}^{(3)})(4k^2n^2g_{402}\cos 2ny + 36l^2m^2g_{420}\cos 2mx)\sin kx\,\sin 3ly\\ &+\gamma_{14}\beta^2(\varepsilon w_1(\tau))^2(\varepsilon^3 A_{31}^{(3)})(36k^2n^2g_{402}\cos 2ny + 4l^2m^2g_{420}\cos 2mx)\sin 3kx\,\sin ly\\ &+g_{42}(\varepsilon w_1(\tau))^3\sin mx\,\sin ny = 0.\end{aligned} \tag{45}$$

Multiplying Eq. (45) by $(\sin mx \sin ny)$ and integrating over the plate area, we obtain

$$g_{43}\frac{\mathrm{d}^2(\varepsilon w_1)}{\mathrm{d}\tau^2} + g_{41}(\varepsilon w_1) + g_{44}(\varepsilon w_1)^2 + g_{42}(\varepsilon w_1)^3 = 0. \tag{46}$$

From Eq. (46), the nonlinear frequency of the plates can be expressed as [23]

$$\omega_{\mathrm{NL}} = \omega_L \left[1 + \frac{9g_{42}g_{41} - 10g_{44}^2}{12g_{41}^2} A^2\right]^{1/2} \quad (P_x \neq P_{\mathrm{cr}}). \tag{47a}$$

$$\omega_{\mathrm{NL}} = \left[\frac{3}{4}\frac{g_{42}}{g_{43}}\right]^{1/2} A \quad (P_x = P_{\mathrm{cr}}), \tag{47b}$$

where $\omega_L = [g_{41}/g_{43}]^{1/2}$ is the dimensionless linear frequency and $A = \bar{W}_{\max}/h$ is the amplitude to thickness ratio. According to Eq. (22), the corresponding linear frequency can be expressed as $\bar{\omega}_L = \omega_L(\pi/a)(E_0/\rho_0)^{1/2}$, where E_0 and ρ_0 are defined as in Eq. (22). From Eq. (47b), it can be seen that the nonlinear frequency varies linearly with the amplitude $\bar{W}_{\max}/h$, when $P_x/P_{\mathrm{cr}} = 1$.

4. Numerical results and discussions

Numerical results are presented in this section for simply supported sandwich plates with FGM face sheets. The material mixture for FGM face sheets is considered to be silicon nitride and stainless steel, referred to as Si_3N_4/SUS304. The material properties P_f, such as Young's modulus E_f, thermal expansion coefficient α_f and thermal conductivity κ_f, can be expressed as a nonlinear function of temperature as (Touloukian [24])

$$P_f = P_0(P_{-1}T^{-1} + 1 + P_1T + P_2T^2 + P_3T^3) \tag{48}$$

in which $T = T_0 + \Delta T$ and $T_0 = 300\,\mathrm{K}$. P_0, P_{-1}, P_1, P_2 and P_3 are the coefficients of temperature T (K) and are unique to the constituent materials. Typical values for Young's modulus E_f (in Pa), thermal expansion coefficient α_f (in K^{-1}) and whose thermal conductivity κ_f (in W/m K) of these materials are listed in Table 1 (from Reddy and Chin [25]). The same metal is selected for the homogeneous substrate, and the material properties are also assumed to be nonlinear functions of temperature of Eq. (48). Poisson's ratio is assumed to be a constant, that is, $v_f = 0.28$ for Si_3N_4/SUS304 face sheets and $v_H = 0.3$ for the SUS304 substrate.

4.1. Comparison studies

To ensure the accuracy and effectiveness of the present method, four test examples were solved for single plates.

Example 1. We first consider the free vibration of an FGM square plate made of aluminum oxide and Ti–6Al–4V. The top surface is ceramic rich, whereas the bottom surface is metal rich. The material properties are: $E_m = 105.7\,\mathrm{GPa}$, $v_m = 0.2981$ and $\rho_m = 4429\,\mathrm{kg/m^3}$ for Ti–6Al–4V, and $E_c = 320.24\,\mathrm{GPa}$, $v_c = 0.26$ and $\rho_c = 3750\,\mathrm{kg/m^3}$ for aluminum oxide. The FGM plate has $a = b = 0.4\,\mathrm{m}$ and $h = 5\,\mathrm{mm}$. Table 2 gives the comparison of natural frequency $\bar{\omega}_L$ (Hz) for the two special cases of isotropy, i.e. volume fraction index

Table 1
Temperature-dependent coefficients for Si_3N_4 and SUS304, from Reddy and Chin [25]

	P_0	P_{-1}	P_1	P_2	P_3
Si_3N_4					
E (Pa)	348.43e+9	0.0	−3.070e−4	2.160e−7	−8.964e−11
α (K^{-1})	5.8723e−6	0.0	9.095e−4	0.0	0.0
κ (W/m K)	13.723	0.0	−1.032e−3	5.466e−7	−7.876e−11
ρ ($\mathrm{kg/m^3}$)	2370	0.0	0.0	0.0	0.0
SUS304					
E (Pa)	201.04e+9	0.0	3.079e−4	−6.534e−7	0.0
α (K^{-1})	12.330e−6	0.0	8.086e−4	0.0	0.0
κ (W/m K)	15.379	0.0	−1.264e−3	2.092e−6	−7.223e−10
ρ ($\mathrm{kg/m^3}$)	8166	0.0	0.0	0.0	0.0

Table 2
Comparisons of natural frequency $\bar{\omega}_L$ (in Hz) for FGM plates with two special values of volume fraction

	$N=0$			$N=2000$		
	He et al. [26]	Park and Kim [12]	Present	He et al. [26]	Park and Kim [12]	Present
1	144.66	145.06	144.96	268.92	274.23	271.08
2	360.53	362.41	362.10	669.40	685.18	677.14
3	360.53	362.41	362.10	669.40	685.18	677.14
4	569.89	579.39	578.86	1052.49	1095.40	1082.54
5	720.57	724.62	723.17	1338.52	1369.98	1352.44
6	720.57	–	723.17	1338.52	–	1352.44
7	919.74	–	939.33	1695.23	–	1756.75
8	919.74	–	939.33	1695.23	–	1756.75
9	1225.72	–	1226.97	2280.95	–	2294.80
10	1225.72	–	1226.97	2280.95	–	2294.80

Table 3
Comparisons of nonlinear frequency ratio (ω_{NL}/ω_L) for a simply supported Si_3N_4/SUS304 plate in ambient temperature field ($a/b=1$, $a/h=10$, $N=5$)

Temperature field	$\bar{W}/h=0.2$	0.4	0.6	0.8	1.0
Uniform temperature field ($T_U=300\,K$, $T_L=300\,K$)					
Sundararajan et al. [27]	1.0110	1.0719	1.1760	1.3139	1.4768
Present	1.0210	1.0832	1.1791	1.3015	1.4437
Non-uniform temperature field ($T_U=400K$, $T_L=300\,K$)					
Sundararajan et al. [27]	1.0125	1.0775	1.1875	1.3318	1.5017
Present	1.0221	1.0860	1.1849	1.3108	1.4567

$N=0$ and 2000. The results of He et al. [26] and Park and Kim [12] are also given for direct comparison. Note that in this example the material properties are assumed to be independent of temperature.

Example 2. We now consider the nonlinear frequency ratio (ω_{NL}/ω_L) for a simply supported Si_3N_4/SUS304 plate in an ambient temperature field. The top surface is ceramic rich, whereas the bottom surface is metal rich. The material properties are the same as those listed in Table 1. The FGM plate has $a/b=1$, $a/h=10$, and the volume fraction index N is taken to be 5. The results are listed in Table 3 and compared with the FEM results of Sundararajan et al. [27]. Note that in Ref. [27], the material properties of the constituents using the Mori–Tanaka homogenization method are given.

Example 3. We then examine the relationship between natural frequency ratio (ω/ω_0) and in-plane compressive load ratio P/P_{cr} for an isotropic rectangular plate with an aspect ratio of 3, where ω_0 is the lowest linear natural frequency of the plate and P_{cr} is the buckling load of the same plate under uniaxial compression. The curves are plotted in Fig. 2 and compared with the FEM result of Yang and Han [4] based on a high-order triangular membrane finite element combined with a fully conforming triangular plate bending element.

Example 4. We finally examine the relationship between fundamental frequencies $\bar{\omega}_L$ (Hz) and temperature increase T (K) for a simply supported Si_3N_4/SUS304 plate under the two special cases of isotropy, i.e. volume fraction index $N=0$ and 2000. The top surface is ceramic rich, whereas the bottom surface is metal rich. The material properties are the same as those listed in Table 1. The FGM plate has $a=b=0.3\,m$ and $a/h=100$. The curves are plotted in Fig. 3 and compared with the FEM result of Park and Kim [12] based on the first-order shear deformation plate theory.

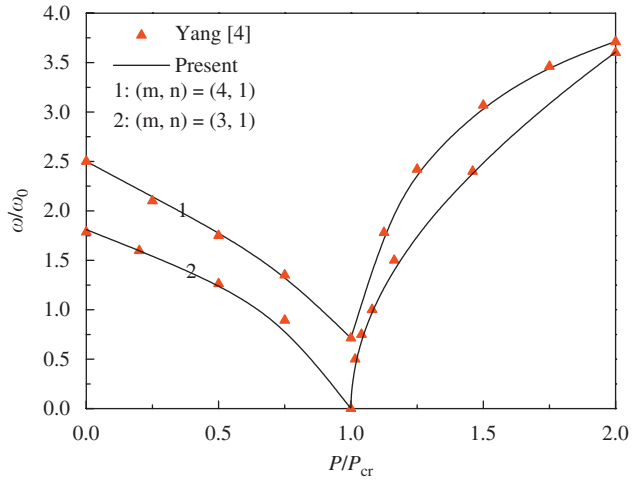

Fig. 2. Comparisons of natural frequencies for the buckled isotropic rectangular plate with aspect ratio of 3 ($\nu = 0.3$).

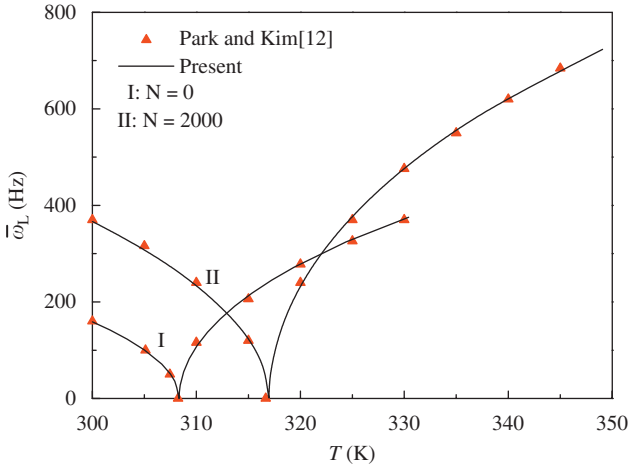

Fig. 3. Comparisons of natural frequencies for the thermally buckled Si_3N_4/SUS304 square plate.

These four comparisons show that the results from the present method are in good agreement with the existing results, thus verifying the reliability and accuracy of the present method.

4.2. Parametric studies

A parametric study has been carried out and typical results are shown in Figs. 4–13. For these examples, the plate geometric parameter $a/b = 1$, $b/h = 20$, and the thickness of the FGM face sheets $h_F = 1$ mm whereas the thickness of the homogeneous substrate is taken to be $h_H = 4$, 6 and 8 mm, so that the substrate-to-face sheet thickness ratio $h_H/h_F = 4$, 6 and 8, respectively. It should be appreciated that in all these examples $m = n = k = l = 1$. $\bar{W}_{\max}/h$ is the amplitude to thickness ratio and the nonlinear frequency ω_{NL} has been normalized by the lowest linear natural frequency ω_0 of the same plate.

Fig. 4 shows the effects of volume fraction index N on the linear fundamental frequencies $\bar{\omega}_L$ of the pre- and post-buckled sandwich plate with $h_H/h_F = 4$ under a uniform or a non-uniform temperature field. It can be seen that as the volume fraction index increases, the fundamental frequency increases in the pre-buckling region, but decreases in the initial post-buckling region ($P_x < 3500$ kN), and in the deep post-buckling region the fundamental frequency becomes greater, when increasing in N. This is due to the fact that the plate

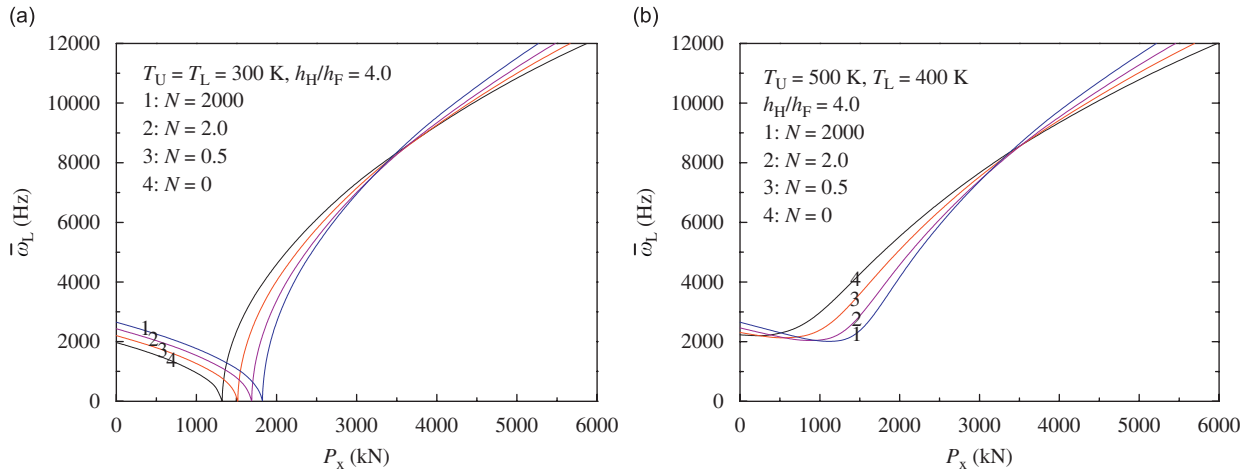

Fig. 4. Effects of volume fraction index N on the fundamental frequencies of the pre- and post-buckled sandwich plate in thermal environments: (a) uniform temperature field; (b) heat conduction.

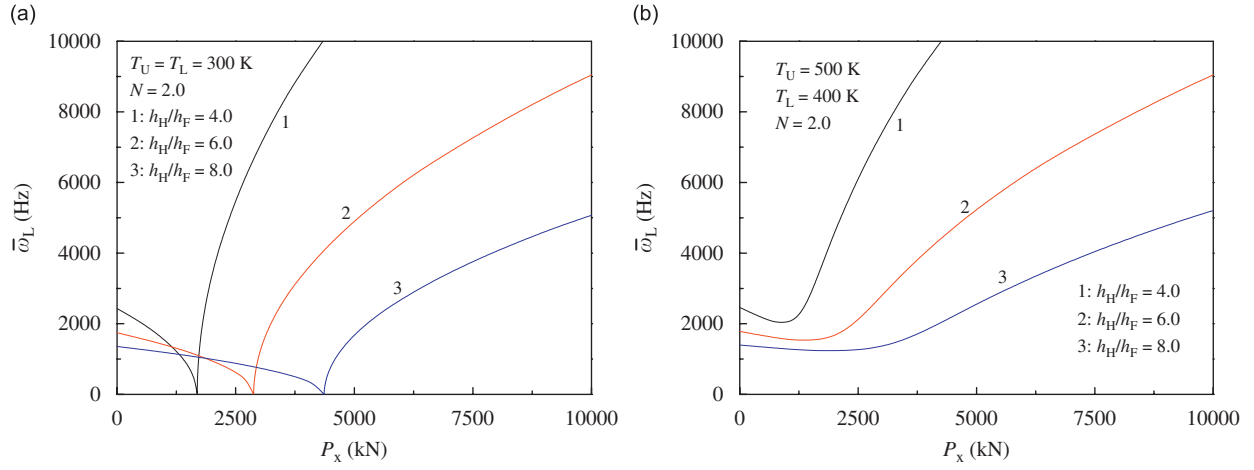

Fig. 5. Effects of substrate-to-face sheet thickness ratio on the fundamental frequencies of the pre- and post-buckled sandwich plate in thermal environments: (a) uniform temperature field; (b) heat conduction.

stiffness is increased in the pre-buckling region, when increasing in N, but in the initial post-buckling region the initial deflection is an important issue and the plate will have a small deflection when it has a great stiffness; further in the deep post-buckling region the effect of plate stiffness becomes more pronounced again.

Fig. 5 shows the effects of substrate-to-face sheet thickness ratio h_H/h_F on the fundamental frequencies of the pre- and post-buckled sandwich plate with $N = 2$ under a uniform or a non-uniform temperature field. It is found that the increase in h_H/h_F yields a decrease in fundamental frequency. This is because the stiffness of the sandwich plate becomes weaker when h_H/h_F is increased.

Fig. 6 shows temperature changes in the fundamental frequencies of the pre- and post-buckled sandwich plate with $h_H/h_F = 4$ and $N = 2$ under a uniform or a non-uniform temperature field. It can be seen that, for a uniform temperature field, as the temperature is increased, fundamental frequencies have decreased in the pre-buckling region, but increased in the post-buckling region. It can also be seen that the effect of the non-uniform temperature field is larger than that of uniform temperature field. When heat conduction is taken into consideration, the larger top–bottom temperature difference leads to a larger fundamental frequency increase.

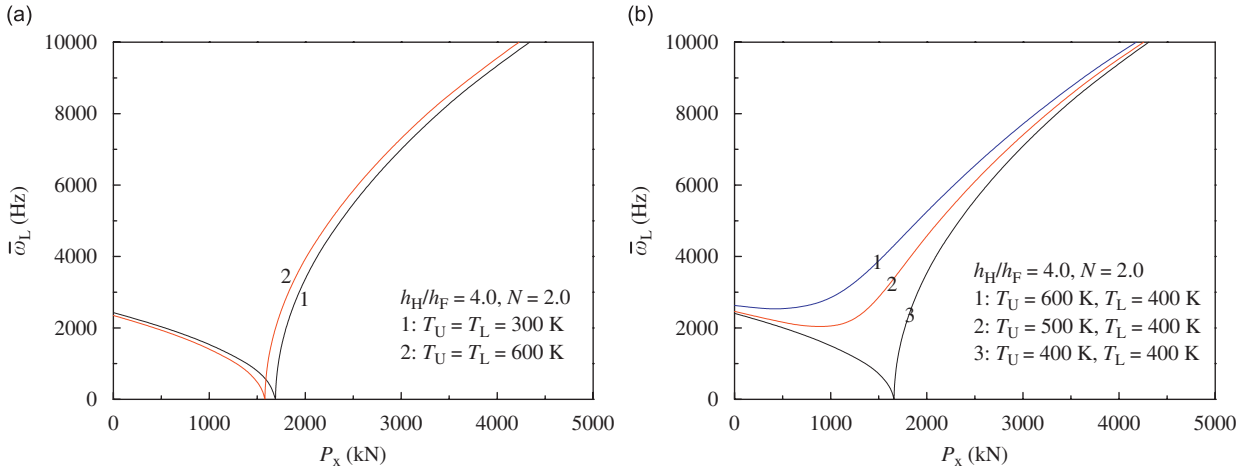

Fig. 6. Effects of temperature changes on the fundamental frequencies of the pre- and post-buckled sandwich plate: (a) uniform temperature field; (b) heat conduction.

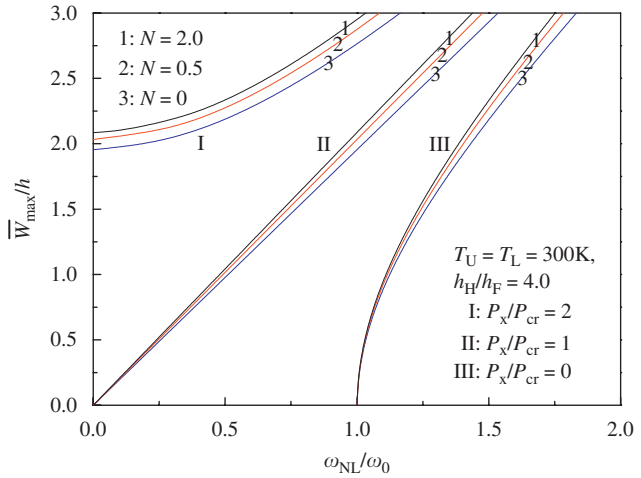

Fig. 7. Effects of volume fraction index N on the nonlinear frequency ratio of the pre- and post-buckled sandwich plate.

From Figs. 4 to 6, it can be seen that, as the compressive load reaches the buckling load, the fundamental frequencies will drop to zero under a uniform temperature field. In contrast, the fundamental frequencies do not go to zero, because no bifurcation-type buckling could occur when heat conduction is taken into account.

Figs. 7–9 show, respectively, the effects of volume fraction index N, substrate-to-face sheet thickness ratio h_H/h_F and temperature changes on the nonlinear frequency ratio of the pre- and post-buckled sandwich plate in thermal environments. Three cases, i.e. $P_x/P_{cr} = 0$, 1 and 2, are considered. $P_x/P_{cr} = 0$ denotes no in-plane loads, $P_x/P_{cr} = 1$ denotes bifurcation buckling case and $P_x/P_{cr} = 2$ represents a large-amplitude free vibration about a post-buckled equilibrium state. Note that in Fig. 9 P_x/P_{cr} is replaced by P_x/P_0, where P_0 is a reference value of buckling load of the plate at $T_U = T_L = 300$ K. It can be seen that the nonlinear frequency ratio is decreased, when the volume fraction index N is increased. The substrate-to-face sheet thickness ratio h_H/h_F and temperature changes only have small effects on the nonlinear frequency ratio of the plate. Note that, in the present study, the solution is based on the assumption that the vibration of the plate is symmetric about the flat position. Another type of motion is possible in which the plate vibrates about a static buckled position on one side of the flat position. Such motion is, however, not considered in the present study.

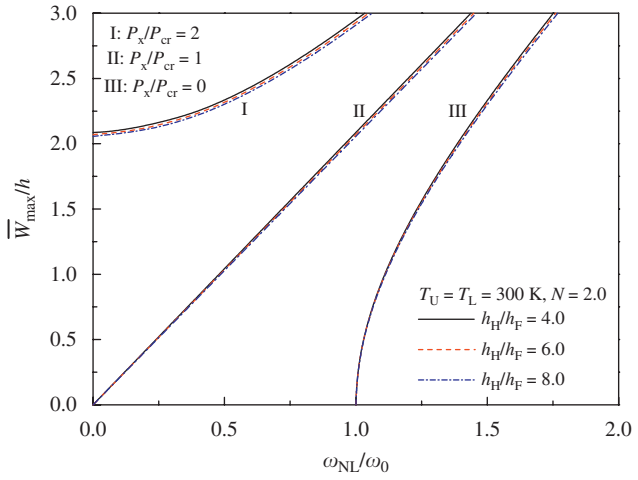

Fig. 8. Effects of substrate-to-face sheet thickness ratio on the nonlinear frequency ratio of the pre- and post-buckled sandwich plate.

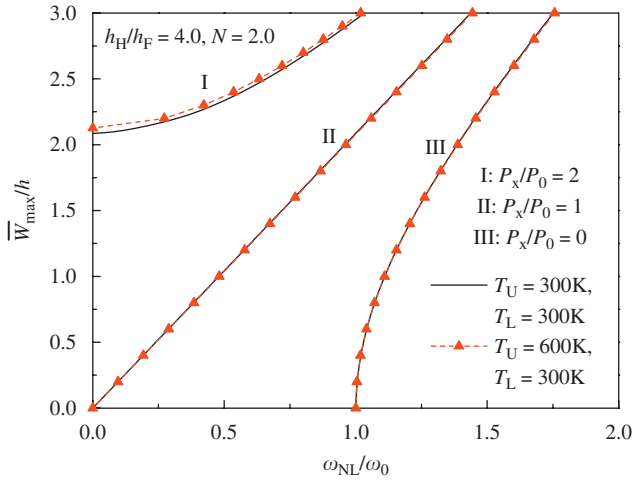

Fig. 9. Effects of temperature changes on the nonlinear frequency ratio of the pre- and post-buckled sandwich plate.

Figs. 10–13 show thermally post-buckled vibration results for the same plate analogous to the compressively post-buckled vibration results of Figs. 4, 5, 7 and 8, which are for the thermal loading case of a uniform temperature field. To compare Figs. 5a and 11, it can be seen that now the buckling temperature is decreased, on increasing t_H/t_F. Otherwise, they lead to broadly the same conclusions as do Figs. 4, 7 and 8.

5. Concluding remarks

Small- and large-amplitude vibration analyses of compressively and thermally post-buckled sandwich plates with FGM face sheets in a thermal environment have been presented. Analytical solutions have been presented by using an improved perturbation technique. Numerical calculations have been performed for mid-plane symmetric sandwich plates with FGM face sheets subjected to uniaxial compression and/or thermal loading. A parametric study with different values of volume fraction index, substrate-to-face sheet thickness ratio and temperature changes have been carried out. Numerical results show that, as the volume fraction index increases, the fundamental frequency increases in the pre-buckling region, but decreases in the post-buckling region. In contrast, the nonlinear frequency ratio decreases in both the pre- and the post-buckling

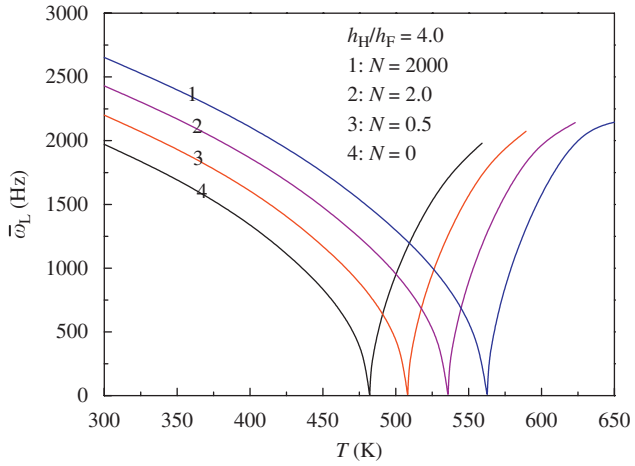

Fig. 10. Effects of volume fraction index N on the fundamental frequencies of the thermally pre- and post-buckled sandwich plate.

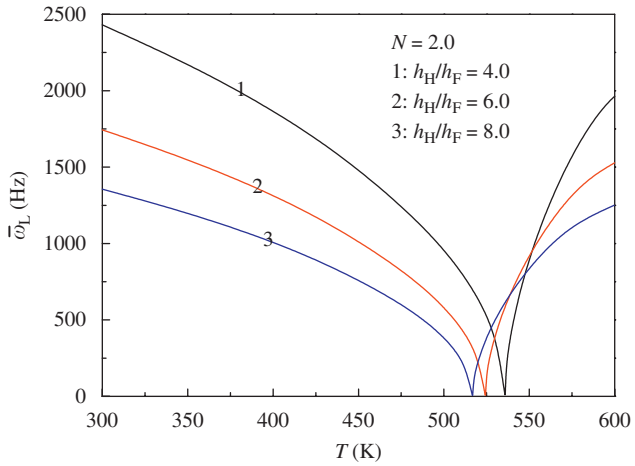

Fig. 11. Effects of substrate-to-face sheet thickness ratio on the fundamental frequencies of the thermally pre- and post-buckled sandwich plate.

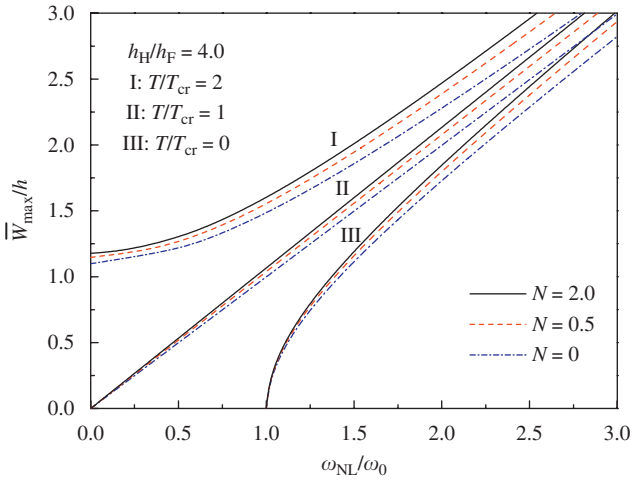

Fig. 12. Effects of volume fraction index N on the nonlinear frequency ratio of the thermally pre- and post-buckled sandwich plate.

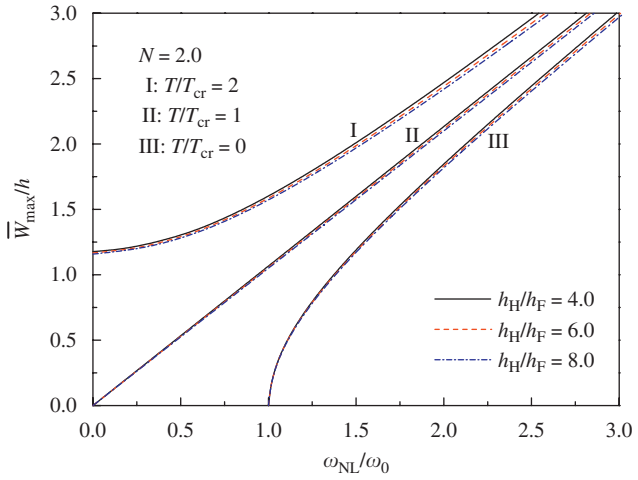

Fig. 13. Effects of substrate-to-face sheet thickness ratio on the nonlinear frequency ratio of the thermally pre- and post-buckled sandwich plate.

region on increasing N. The results reveal that the substrate-to-face sheet thickness ratio and temperature changes have a significant effect on the fundamental frequency, but only have a small effect on the nonlinear frequency ratio.

Appendix A

$$g_{11}^{(i,j)}=\frac{k_{23}^{(i,j)}k_{31}^{(i,j)}-k_{33}^{(i,j)}k_{21}^{(i,j)}}{k_{22}^{(i,j)}k_{33}^{(i,j)}-k_{32}^{(i,j)}k_{23}^{(i,j)}},\quad g_{21}^{(i,j)}=\frac{k_{22}^{(i,j)}k_{31}^{(i,j)}-k_{32}^{(i,j)}k_{21}^{(i,j)}}{k_{23}^{(i,j)}k_{32}^{(i,j)}-k_{33}^{(i,j)}k_{22}^{(i,j)}},$$

$$g_{31}^{(i,j)}=a_1^{(i,j)}+b_1^{(i,j)}g_{11}^{(i,j)}+c_1^{(i,j)}g_{21}^{(i,j)},$$

$$g_{402}=\frac{\gamma_{24}m^2n^2\beta^2}{2\left(16\gamma_{214}n^4\beta^4+\dfrac{64\gamma_{14}\gamma_{24}\gamma_{223}^2n^6\beta^6}{\gamma_{41}+4\gamma_{432}n^2\beta^2}\right)},\quad g_{420}=\frac{\gamma_{24}m^2n^2\beta^2}{2\left(16m^4+\dfrac{64\gamma_{14}\gamma_{24}\gamma_{220}^2m^6}{\gamma_{31}+4\gamma_{320}m^2}\right)},$$

$$g_{12}=-\frac{8\gamma_{220}\gamma_{14}m^3}{\gamma_{31}+4\gamma_{320}m^2}g_{420},\quad g_{22}=-\frac{8\gamma_{233}\gamma_{14}n^3\beta^3}{\gamma_{41}+4\gamma_{432}n^2\beta^2}g_{402},$$

$$g_{441}=8g_{12}\gamma_{120}m^3+16g_{420}\gamma_{14}\gamma_{140}m^4+g_{31}^{(1,1)}\gamma_{14}\beta^2m^2n^2,$$

$$g_{442}=8g_{22}\gamma_{133}n^3\beta^3+16g_{420}\gamma_{14}\gamma_{144}n^4\beta^4+g_{31}^{(1,1)}\gamma_{14}\beta^2m^2n^2,$$

$$g_{331}=\frac{2\gamma_{14}m^2n^2\beta^2}{k_{11}^{(3,1)}+k_{12}^{(3,1)}g_{11}^{(3,1)}+k_{13}^{(3,1)}g_{21}^{(3,1)}-\gamma_{14}\beta^2(9m^2g_{xxk1}+n^2g_{xxk2}+s^{(3,1)})}g_{420},$$

$$g_{313}=\frac{2\gamma_{14}m^2n^2\beta^2}{k_{11}^{(1,3)}+k_{12}^{(1,3)}g_{11}^{(1,3)}+k_{13}^{(1,3)}g_{21}^{(1,3)}-\gamma_{14}\beta^2(m^2g_{xxk1}+9n^2g_{xxk2}+s^{(1,3)})}g_{402},$$

$$g_1=\frac{b_3(k_{12}^{(1,1)}k_{23}^{(1,1)}-k_{22}^{(1,1)}k_{13}^{(1,1)})-b_2(k_{12}^{(1,1)}k_{33}^{(1,1)}-k_{13}^{(1,1)}k_{32}^{(1,1)})}{g_{xxk3}},$$

$$g_2=\frac{b_2(k_{11}^{(1,1)}k_{33}^{(1,1)}-k_{13}^{(1,1)}k_{31}^{(1,1)})-b_3(k_{11}^{(1,1)}k_{23}^{(1,1)}-k_{13}^{(1,1)}k_{21}^{(1,1)})}{g_{xxk3}},$$

$$g_3=-\frac{k_{11}^{(1,1)}g_1+k_{12}^{(1,1)}g_2}{k_{13}^{(1,1)}},\quad g_4=a_1^{(1,1)}g_1+b_1^{(1,1)}g_2+c_1^{(1,1)}g_3,$$

$$
\begin{aligned}
g_{41} &= k_{11}^{(1,1)} + k_{12}^{(1,1)} g_{11}^{(1,1)} + k_{13}^{(1,1)} g_{21}^{(1,1)} - \gamma_{14}\beta^2 (m^2 g_{xxk1} + n^2 g_{xxk2} + s^{(1,1)}),\\
g_{42} &= 2\gamma_{14}\beta^2 m^2 n^2 (g_{402} + g_{420}),\\
g_{43} &= -\left(\gamma_{170} - \gamma_{171} m^2 - \gamma_{171} n^2 \beta^2 - \gamma_{80} m g_{11}^{(1,1)} - \gamma_{80} n\beta g_{21}^{(1,1)}\right),\\
g_{44} &= -\frac{2}{\pi^2 mn}\left[g_{441}(1-\cos n\pi)\left(\frac{2}{3}+\frac{1}{3}\cos 3m\pi - \cos m\pi\right) + g_{442}(1-\cos m\pi)\left(\frac{2}{3}+\frac{1}{3}\cos 3n\pi - \cos n\pi\right)\right],
\end{aligned}
\tag{A.1}
$$

where

$$
\begin{aligned}
s^{(i,j)} = \frac{2}{\pi^2}\Bigg\{ & \left[2(k^2n^2 + l^2m^2)\left(\frac{1}{k} - \frac{1}{2k+4m} - \frac{1}{2k-4m}\right)\left(\frac{1}{l} - \frac{1}{2l+4n} - \frac{1}{2l-4n}\right)\right.\\
& \left. -mnkl\left(\frac{1}{2m+k} + \frac{1}{2m-k}\right)\left(\frac{1}{2n+l} + \frac{1}{2n-l}\right)\right](\varepsilon A_{11}^{(1)}) + \left[2(k^2n^2 + 9l^2m^2)\right.\\
& \times \left(\frac{1}{k} - \frac{1}{2k+4m} - \frac{1}{2k-4m}\right)\left(\frac{1}{3l} - \frac{1}{6l+4n} - \frac{1}{6l-4n}\right)\\
& \left. - 3mnkl\left(\frac{1}{2m+k} + \frac{1}{2m-k}\right)\left(\frac{1}{2n+3l} + \frac{1}{2n-3l}\right)\right](\varepsilon^3 A_{13}^{(3)}) + \left[2(9k^2n^2 + l^2m^2)\right.\\
& \times \left(\frac{1}{3k} - \frac{1}{6k+4m} - \frac{1}{6k-4m}\right)\left(\frac{1}{l} - \frac{1}{2l+4n} - \frac{1}{2l-4n}\right)\\
& \left. - 3mnkl\left(\frac{1}{2m+3k} + \frac{1}{2m-3k}\right)\left(\frac{1}{2n+l} + \frac{1}{2n-l}\right)\right](\varepsilon^3 A_{31}^{(3)})\Bigg\} g_{31}^{(i,j)},\\
b_2 = \gamma_{90} m + \gamma_{10} g_{11}^{(1,1)}, \quad & b_3 = \gamma_{90} n\beta + \gamma_{10} g_{21}^{(1,1)},\\
g_{xxk1} = B_{00}^{(0)} + \varepsilon^2 B_{00}^{(2)} + \varepsilon^4 B_{00}^{(4)}, \quad & g_{xxk2} = b_{00}^{(0)} + \varepsilon^2 b_{00}^{(2)} + \varepsilon^4 b_{00}^{(4)},\\
g_{xxk3} = & k_{11}^{(1,1)} k_{22}^{(1,1)} k_{33}^{(1,1)} + k_{12}^{(1,1)} k_{23}^{(1,1)} k_{31}^{(1,1)} + k_{21}^{(1,1)} k_{32}^{(1,1)} k_{13}^{(1,1)},\\
& - k_{23}^{(1,1)} k_{32}^{(1,1)} k_{11}^{(1,1)} - k_{22}^{(1,1)} k_{31}^{(1,1)} k_{13}^{(1,1)} - k_{21}^{(1,1)} k_{12}^{(1,1)} k_{33}^{(1,1)},\\
g_{xxk4} = & -\frac{\gamma_{24}}{m^4 + 2\gamma_{212}(im)^2(jn)^2\beta^2 + \gamma_{214}(jn)^4\beta^4}.
\end{aligned}
\tag{A.2}
$$

In the above equations

$$
\begin{aligned}
k_{11}^{(i,j)} &= \gamma_{110}(im)^4 + 2\gamma_{112}(im)^2(jn)^2\beta^2 + \gamma_{114}(jn)^4\beta^4 + \gamma_{14}[\gamma_{140}(im)^4 + \gamma_{142}(im)^2(jn)^2\beta^2\\
&\quad + \gamma_{144}(jn)^4\beta^4] a_1^{(i,j)},\\
k_{12}^{(i,j)} &= -[\gamma_{120}(im)^3 + \gamma_{122} im(jn)^2\beta^2] + \gamma_{14}[\gamma_{140}(im)^4 + \gamma_{142}(im)^2(jn)^2\beta^2 + \gamma_{144}(jn)^4\beta^4] b_1^{(i,j)},\\
k_{13}^{(i,j)} &= -[\gamma_{131}(im)^2 jn\beta + \gamma_{133}(jn)^3\beta^3] + \gamma_{14}[\gamma_{140}(im)^4 + \gamma_{142}(im)^2(jn)^2\beta^2 + \gamma_{144}(jn)^4\beta^4] c_1^{(i,j)},\\
k_{21}^{(i,j)} &= \gamma_{31} im - \gamma_{310}(im)^3 - \gamma_{312} im(jn)^2\beta^2 - \gamma_{14}[\gamma_{220}(im)^3 + \gamma_{222}(im)(jn)^2\beta^2] a_1^{(i,j)},\\
k_{22}^{(i,j)} &= \gamma_{31} + r_{320}(im)^2 + \gamma_{322}(jn)^2\beta^2 - \gamma_{14}[\gamma_{220}(im)^3 + \gamma_{222}(im)(jn)^2\beta^2] b_1^{(i,j)},\\
k_{23}^{(i,j)} &= \gamma_{331}(im)(jn)\beta - \gamma_{14}[\gamma_{220}(im)^3 + \gamma_{222}(im)(jn)^2\beta^2] c_1^{(i,j)},\\
k_{31}^{(i,j)} &= \gamma_{41} jn\beta - \gamma_{411}(im)^2 jn\beta - \gamma_{413}(jn)^3\beta^3 - \gamma_{14}[\gamma_{231}(im)^2(jn)\beta + \gamma_{233}(jn)^3\beta^3] a_1^{(i,j)},\\
k_{32}^{(i,j)} &= \gamma_{331}(im)(jn)\beta - \gamma_{14}[\gamma_{231}(im)^2(jn)\beta + \gamma_{233}(jn)^3\beta^3] b_1^{(i,j)},\\
k_{33}^{(i,j)} &= \gamma_{41} + r_{430}(im)^2 + \gamma_{432}(jn)^2\beta^2 - \gamma_{14}[\gamma_{231}(im)^2(jn)\beta + \gamma_{233}(jn)^3\beta^3] c_1^{(i,j)}.
\end{aligned}
\tag{A.3}
$$

$$
\begin{aligned}
b_1^{(i,j)} &= -\frac{\gamma_{24}[\gamma_{220}(im)^3+\gamma_{222}(im)(jn)^2\beta^2]}{m^4+2\gamma_{212}(im)^2(jn)^2\beta^2+\gamma_{214}(jn)^4\beta^4},\\
c_1^{(i,j)} &= -\frac{\gamma_{24}[\gamma_{231}(im)^2(jn)\beta+\gamma_{233}(jn)^3\beta^3]}{m^4+2\gamma_{212}(im)^2(jn)^2\beta^2+\gamma_{214}(jn)^4\beta^4},\\
a_1^{(i,j)} &= g_{xxk4}\times[\gamma_{240}(im)^4+\gamma_{242}(im)^2(jn)^2\beta^2+\gamma_{244}(jn)^4\beta^4]\\
&\quad+g_{xxk4}\times\frac{2\beta^2}{\pi^2}\left\{\left[2(k^2n^2+l^2m^2)\left(\frac{1}{k}-\frac{1}{2k+4m}-\frac{1}{2k-4m}\right)\left(\frac{1}{l}-\frac{1}{2l+4n}-\frac{1}{2l-4n}\right)\right.\right.\\
&\quad\left.-mnkl\left(\frac{1}{2m+k}+\frac{1}{2m-k}\right)\left(\frac{1}{2n+l}+\frac{1}{2n-l}\right)\right](\varepsilon A_{11}^{(1)})+\left[2(k^2n^2+9l^2m^2)\right.\\
&\quad\times\left(\frac{1}{k}-\frac{1}{2k+4m}-\frac{1}{2k-4m}\right)\left(\frac{1}{3l}-\frac{1}{6l+4n}-\frac{1}{6l-4n}\right)\\
&\quad\left.-3mnkl\left(\frac{1}{2m+k}+\frac{1}{2m-k}\right)\left(\frac{1}{2n+3l}+\frac{1}{2n-3l}\right)\right](\varepsilon^3A_{13}^{(3)})+\left[2(9k^2n^2+l^2m^2)\right.\\
&\quad\times\left(\frac{1}{3k}-\frac{1}{6k+4m}-\frac{1}{6k-4m}\right)\left(\frac{1}{l}-\frac{1}{2l+4n}-\frac{1}{2l-4n}\right)\\
&\quad\left.\left.-3mnkl\left(\frac{1}{2m+3k}+\frac{1}{2m-3k}\right)\left(\frac{1}{2n+l}+\frac{1}{2n-l}\right)\right](\varepsilon^3A_{31}^{(3)})\right\}. \qquad \text{(A.4)}
\end{aligned}
$$

References

[1] J. Yang, H.-S. Shen, L. Zhang, Nonlinear local response of foam-filled sandwich plates with laminated faces under combined transverse and in-plane loads, *Composite Structures* 52 (2001) 137–148.

[2] A.K. Nayak, S.S.J. Moy, R.A. Shenoi, A higher order finite element theory for buckling and vibration analysis of initially stressed composite sandwich plates, *Journal of Sound and Vibration* 286 (2005) 763–780.

[3] R.L. Bisplinghoff, T.H.H. Pian, On the vibration of thermally buckled bars and plates, *Proceedings of the Ninth International Congress for Applied Mechanics*, Vol. 7, 1957, pp. 307–318.

[4] T.Y. Yang, A.D. Han, Buckled plate vibrations and large amplitude vibrations using high-order triangular elements, *AIAA Journal* 21 (1983) 758–766.

[5] R.C. Zhou, D.Y. Xue, C. Mei, C.C. Gray, Vibration of thermally buckled composite plates with initial deflections using triangular elements, in: *Thirty-forth AIAA/ASME/ASCE/AHS/ASC Structures, Structural Dynamics and Materials Conference*, part 1, 1993, pp. 226–235.

[6] D.-M. Lee, I. Lee, Vibration behaviors of thermally postbuckled anisotropic plates using first-order shear deformable plate theory, *Computers and Structures* 63 (1997) 371–378.

[7] D.-M. Lee, I. Lee, Vibration analysis of stiffened laminated plates including thermally postbuckled deflection effect, *Journal of Reinforced Plastics and Composites* 16 (1997) 1138–1154.

[8] L.-C. Shiau, T.-Y. Wu, Free vibration of buckled laminated plates by finite element method, *Journal of Vibration and Acoustics—Transactions of the ASME* 119 (1997) 635–640.

[9] L.-C. Shiau, S.-Y. Kuo, Free vibration of thermally buckled composite sandwich plates, *Journal of Vibration and Acoustics—Transactions of the ASME* 128 (2006) 1–7.

[10] J. Girish, L.S. Ramachandra, Thermal postbuckled vibrations of symmetrically laminated composite plates with initial geometric imperfections, *Journal of Sound and Vibration* 282 (2005) 1137–1153.

[11] M.K. Singha, L.S. Ramachandra, J.N. Bandyopadhyay, Vibration behavior of thermally stressed composite skew plate, *Journal of Sound and Vibration* 296 (2006) 1093–1102.

[12] J.S. Park, J.H. Kim, Thermal postbuckling and vibration analyses of functionally graded plates, *Journal of Sound and Vibration* 289 (2006) 77–93.

[13] L. Librescu, S.-Y. Oh, O. Song, Thin-walled beams made of functionally graded materials and operating in a high temperature environment: vibration and stability, *Journal of Thermal Stresses* 28 (2005) 649–712.

[14] J.N. Reddy, A simple higher-order theory for laminated composite plates, *Journal of Applied Mechanics—Transactions of the ASME* 51 (1984) 745–752.

[15] J.N. Reddy, A refined nonlinear theory of plates with transverse shear deformation, *International Journal of Solids and Structures* 20 (1984) 881–896.

[16] H.-S. Shen, Kármán-type equations for a higher-order shear deformation plate theory and its use in the thermal postbuckling analysis, *Applied Mathematics and Mechanics* 18 (1997) 1137–1152.

[17] H.-S. Shen, Nonlinear bending response of functionally graded plates subjected to transverse loads and in thermal environments, *International Journal of Mechanical Sciences* 44 (2002) 561–584.
[18] H.-S. Shen, Thermal postbuckling behavior of shear deformable FGM plates with temperature-dependent properties, *International Journal of Mechanical Sciences* 49 (2007) 466–478.
[19] X.-L. Huang, H.-S. Shen, Nonlinear vibration and dynamic response of functionally graded plates in thermal environments, *International Journal of Solids and Structures* 41 (2004) 2403–2427.
[20] X.-L. Huang, J.-J. Zheng, Nonlinear vibration and dynamic response of simply supported shear deformable laminated plates on elastic foundations, *Engineering Structures* 25 (2003) 1107–1119.
[21] H.-S. Shen, S.-R. Li, Postbuckling of sandwich plates with FGM face sheets and temperature-dependent properties, *Composites Part B: Engineering* 39 (2) (2008) 332–344.
[22] H.-S. Shen, Thermal buckling and postbuckling of laminated plates, in: N.E. Shanmugam, C.M. Wang (Eds.), *Analysis and Design of Plated Structures (Vol. 1: Stability)*, Woodhead Publishing Ltd., 2006, pp. 170–213.
[23] H.-Q. Wang, *Nonlinear Vibration*, Higher Education Press, 1992 (in Chinese).
[24] Y.S. Touloukian, *Thermophysical Properties of High Temperature Solid Materials*, Macmillan, New York, 1967.
[25] J.N. Reddy, C.D. Chin, Thermomechanical analysis of functionally graded cylinders and plates, *Journal of Thermal Stresses* 21 (1998) 593–629.
[26] X.Q. He, T.Y. Ng, S. Sivashanker, K.M. Liew, Active control of FGM plates with integrated piezoelectric sensors and actuators, *International Journal of Solids and Structures* 38 (2001) 1641–1655.
[27] N. Sundararajan, T. Prakash, M. Ganapathi, Nonlinear free flexural vibrations of functionally graded rectangular and skew plates under thermal environments, *Finite Elements in Analysis and Design* 42 (2005) 152–168.